# Quantitative Prediction of On-chip Capacitive and Inductive Crosstalk Noise and Discussion on Wire Cross-Sectional Area Toward Inductive Crosstalk Free Interconnects

Yasuhiro Ogasahara, Masanori Hashimoto, and Takao Onoye
Dept. Information Systems Engineering, Osaka University, Suita 565-0871, JAPAN
{ogshr,hasimoto,onoye}@ist.osaka-u.ac.jp

*Abstract*— **Capacitive and inductive crosstalk noises are expected to be more serious in advanced technologies. However, capacitive and inductive crosstalk noises in the future have not been concurrently and sufficiently discussed quantitatively, though capacitive crosstalk noise has been intensively studied solely as a primary factor of interconnect delay variation. This paper quantitatively predicts the impact of capacitive and inductive crosstalk in prospective processes, and reveals that interconnect scaling strategies strongly affect relative dominance between capacitive and inductive coupling. Our prediction also makes the point that the interconnect resistance significantly influences both inductive coupling noise and propagation delay. We then evaluate a tradeoff between wire cross-sectional area and worst-case propagation delay focusing on inductive coupling noise, and show that an appropriate selection of wire cross-section can reduce delay uncertainty by the small sacrifice of propagation delay.**

## I. Introduction

In nano-meter technologies, interconnect delay dominates gate delay and accurate estimation of interconnect delay has become an important design issue. Capacitive and inductive crosstalk is a well-known obstacle for accurate interconnect delay estimation. Capacitive crosstalk is widely considered in current designs, whereas inductive crosstalk noise emerges in recent processes. Qualitative discussion generally shows that both capacitive and inductive crosstalk noises will be more significant as the fabrication processes advance, though a paper reports that impact of capacitive crosstalk is reduced in most of shortened interconnects [1]. Technology advancement increases capacitive crosstalk noise owning to a larger aspect ratio of interconnects and sharper signal transition waveforms. In wide and fat global interconnects, fast transitions including higher signal frequency strengthen inductive crosstalk effect.

Crosstalk noise has been widely discussed based on formulas and simulations [1]–[3], and verified with measurement results [4]–[6]. However, a quantitative prediction clearly focusing on relative dominance between capacitive and inductive crosstalk noise in the future has not been reported, as far as the authors know, in spite of its increasing importance.

The contributions of this paper are summarized as follows: 1) predicting capacitive and inductive crosstalk noises in future processes and 2) revealing that delay uncertainty due to inductive coupling can be mitigated by adjusting wire cross-sectional area with a small delay penalty.

This paper quantitatively predicts the impact of capacitive and inductive crosstalk noise in predictive technologies with circuit simulation. We assume that process parameters, such as transistor performance and power supply voltage, follow ITRS prediction [7], [8].

We also evaluate a tradeoff between wire cross-sectional area and propagation delay focusing on inductive coupling noise, because the prediction suggests that the interconnect resistance significantly influences both inductive coupling noise and propagation delay. There are several past works for crosstalk reduction that discuss adjusting interconnect spacing for capacitive noise [9], differential signaling [10], and noise immunity design in a processor design [11]. We, in this paper, focus on mitigation of inductive crosstalk effect by narrowing/widening interconnect. A careful selection of wire cross-section reduces inductive coupling without much degrading the worst-case propagation delay. The advantage is that the cross-sectional area tuning makes consideration of inductive coupling unnecesary without modified design procedure and new design tools.

The remaining of this paper is organized as follows. Section II qualitatively discusses crosstalk noise on global interconnects. Section III describes assumed scenarios of technology advance for crosstalk prediction. Section IV presents quantitative prediction of capacitive and inductive crosstalk. Section V discusses wire cross-section and crosstalk-induced delay. Finally section VI concludes this paper.

## II. Qualitative discussion on crosstalk noise

In this section, we explain transmission line effects of interconnects. The characteristics of capacitive and inductive crosstalk noise and their increase due to process scaling are also described.

### A. Transmission line effects of global interconnects

Transmission line effects should be considered in a long interconnect when signal rise time is short [12]. The interconnect considered as a transmission line is represented as an RC or RLC distributed circuit in circuit simulation, and its current return path has to be appropriately modeled for RL extraction. An approach to determine driver size is impedance matching between driver output resistance and interconnect characteristic impedance. When the characteristic impedance

1-4244-9707-X/06/$20.00 ©2006 IEEE

is equal to the driver resistance and the driver is a CMOS gate, 50% of supply voltage is injected to the interconnect. MOS termination, which is open-end when the receiver is a CMOS gate, doubles the voltage at the end of the interconnect, and a sufficient voltage to sense is input to the receiver. Signal attenuation is also an important characteristic for a long interconnect. The injected signal is attenuated to $e^{-\alpha l}$, where $\alpha$ is attenuation constant and $l$ is interconnect length.

### *B. Crosstalk noise and process advancement*

Capacitive crosstalk arises from a coupling capacitance between interconnects. In the case of two coupled interconnects as shown in Fig. 1, a signal transition on one interconnect induces a voltage fluctuation on another interconnect. The induced noise voltage $v_{noise}$ is roughly expressed as $v_{noise} = RC_C \cdot dV/dt$, where $C_C$ is a coupling capacitance between two interconnects, and $R$ is resistance between the noise observation point and the ideal voltage source including interconnect resistance and driver resistance. Improvement of transistor performance by process advancement increases $dV/dt$, which results in deterioration of capacitive crosstalk noise. In the case of the equivalent circuit of Fig. 1, the peak voltage of capacitive crosstalk noise $v_{max}$ is approximately expressed by Eq. (1) [13].

$$v_{max} = \frac{RC_C \cdot v_{dd}}{R(C + C_C) + t_r/2}, \quad (1)$$

where, $t_r$ is the signal rise time at the aggressor. Equation (1) shows that the noise peak voltage becomes large, but not drastically with respect to $dV/dt$ (=$v_{dd}/t_r$) increase. Reduced interconnect spacing and enlarged aspect ratio of interconnects with technology advance are factors of coupling capacitance increment. These qualitative arguments indicate that capacitive crosstalk noise will be severer in the future.

Inductive crosstalk comes from a mutual inductance between interconnects. Assuming two coupled symmetric interconnects, current variation on one interconnect causes a voltage fluctuation on another interconnect, which is explained with an equation $v_{noise} = M \cdot dI/dt$. $M$ denotes mutual inductance. Higher signal frequency due to technology progress, that is larger $dI/dt$, makes the effect of inductive crosstalk significant. On the other hand, interconnect scaling increases interconnect resistance and characteristic impedance of the interconnect. Large characteristic impedance decreases current flowing in the interconnect and mitigates the effect of inductive crosstalk. Inductive coupling is hardly shielded by signal lines and spreads to wide area, which is different from capacitive coupling. Inductive crosstalk noise is caused by many aggressors, and their noises are superposed, though capacitive crosstalk noise is caused by only adjacent interconnects.

Figure 2 shows an example of noise waveform in the case that capacitive and inductive crosstalk noises simultaneously appear. Supposing two lossless coupled transmission lines, the propagating voltage wave is represented as the sum of even and odd mode waves [2]. The times of flight for capacitive and inductive coupling are given by the Eqs. (2) and (3) respectively.

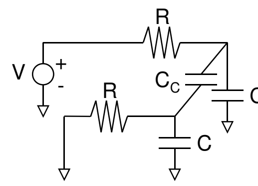


Fig. 1. Equivalent circuit of two symmetric coupled interconnects.

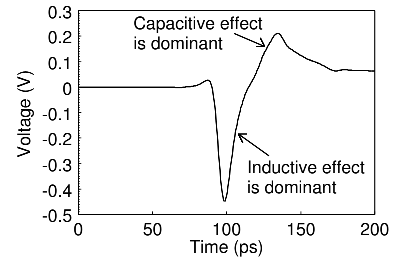


Fig. 2. An example of crosstalk noise waveform.

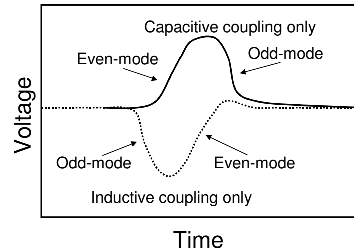


Fig. 3. Conceptual crosstalk noise waveform considering either only capacitive coupling or only inductive coupling.

$$\begin{aligned} t_{C_C even} &= l\sqrt{CL} \\ t_{C_C odd} &= l\sqrt{(C + 2C_C)L} \end{aligned} \quad (2)$$

$$\begin{aligned} t_{M even} &= l\sqrt{C(L + M)} \\ t_{M odd} &= l\sqrt{C(L - M)} \end{aligned} \quad (3)$$

where $l$ is interconnect length and $L$ is self inductance of the interconnect. The even mode wave for inductive coupling travels faster than the other waves and inductive crosstalk appears first as depicted in Fig 3. Capacitive and inductive crosstalk noises are opposite in voltage to each other, and they somewhat cancel each other, which results in the waveform that a capacitive crosstalk nose follows an inductive crosstalk noise as shown in Fig. 2. In this paper, we call the noise waveform where capacitive crosstalk is dominant as "capacitive crosstalk noise", and the noise waveform where inductive crosstalk is dominant as "inductive crosstalk noise", as labeled in Fig. 2.

## III. Scenarios of process advance and simulation setup

This paper predicts influence of capacitive and inductive crosstalk based on circuit simulation. In this section, we show two scenarios of process scaling. Simulation setup, which includes interconnect structure, is also described.

### *A. Assumed scenario*

We assume the two following scenarios of process advancement for 90nm, 65nm, 45nm, and 32nm processes.

Scenario 1

Interconnect cross-section, transistor performance, supply voltage, and dielectric constant of insulator follow ITRS [7], [8] prediction.

TABLE I
PROCESS PARAMETERS IN Scenario 1.
'/' SEPARATES THE PARAMETERS OF S=W / S=4W.

| Process | 90nm | 65nm | 45nm | 32nm |
|---|---|---|---|---|
| Signal rise time(ps) | 25.0 | 15.6 | 10.0 | 6.3 |
| Supply voltage(V) | 1.2 | 1.1 | 1.0 | 0.9 |
| Relative dielectric const. | 3.3 | 2.8 | 2.6 | 2.2 |
| Interconnect width($\mu$m) | 1.00 | 0.67 | 0.49 | 0.35 |
| Interconnect spacing($\mu$m) | 1.00/4.00 | 0.67/2.68 | 0.49/1.96 | 0.35/1.39 |
| Interconnect thickness($\mu$m) | 0.90 | 0.64 | 0.49 | 0.34 |
| Num. of division | 9/9 | 14/13 | 21/19 | 35/30 |
| Characteristic impedance($\Omega$) | 121/138 | 139/168 | 149/180 | 180/214 |

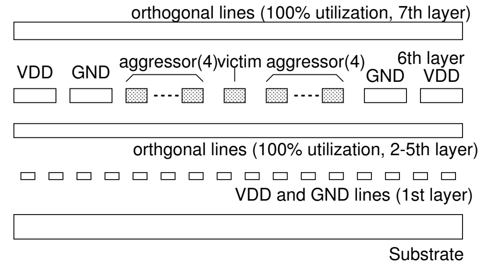

Fig. 4. Interconnect structure for RLC extraction and circuit simulation.

Scenario 2

Interconnect cross-section is unchanged, whereas transistor performance, supply voltage, and dielectric constant of insulator follow ITRS [7], [8] prediction similar to Scnenario 1.

Scenario 2 assumes that a thick metal layer is provided for high-speed interconnection and power distribution. We therefore keep the wire cross-section unchanged.

### B. Simulation setup in Scenario 1

In Scenario 1, characteristics of transistor, supply voltage, and dielectric constant come from ITRS prediction. Cross-section of interconnects is scaled down with the ratio described in ITRS roadmap. Table I summarizes the parameters at each technology node in Scenario 1.

The interconnect structure used for crosstalk noise evaluation is shown in Fig. 4. There are eight aggressors and a victim at M6 layer. The victim is placed at the center of aggressors, and power lines locate at both outer sides. In this structure, long-range effect, which is a characteristic unique to inductive coupling, can be evaluated. Orthogonal lines are placed at M2-M5, and M7 layers, and their track utilization ratio is 100%. Power/ground lines at M1 layer run parallel to the bus interconnects. Width and thickness of the bus interconnects are set to 1$\mu$m and 0.9$\mu$m respectively, and scale in proportion to ITRS prediction at 65-32nm processes. The 1$\mu$m-wide interconnects in a 90nm technology correspond to high performance interconnects. As for wire spacing, we use two parameters; S=W and S=4W, where W is interconnect width and S is spacing. In S=W structure, wires are placed densely and capacitive crosstalk noise is significant. On the other hand, in S=4W structure, the spacing is widened so that capacitive crosstalk is suppressed, which is a common technique in current designs. As a result, inductive crosstalk may dominate capacitive crosstalk. The interconnects are 10mm-long and divided with repeaters. We calculate the number of division using Eq. (4) [14]. Equation (4) gives the division number which makes the propagation delay minimum.

$$k = \sqrt{\frac{0.4 R_{int} C_{int}}{0.7 R_0 C_0}}, \quad (4)$$

where $k$ is the number of division, $R_{int}, C_{int}$ are total resistance and capacitance of the interconnect, $R_0, C_0$ are resistance and capacitance of the minimum size inverter in each process.

RLC coupled ladder model is adopted as an interconnect model for circuit simulation. Resistance, capacitance, and inductance of interconnects are extracted with a 3D field solver [15] considering skin effect. Orthogonal lines at upper and lower layers and the substrate are considered in capacitance extraction. Return current is assumed to flow only in parallel power/ground lines at M6 and M1 layers in inductance and resistance extraction. Resistance and inductance of interconnects are frequency dependent, and values at significant frequency [12] are chosen. Significant frequencies of 90nm, 65nm, 45nm, and 32nm processes are 13.6GHz, 21.8GHz, 34GHz, and 54GHz respectively. Drivers of interconnects are CMOS inverters, and the size is chosen such that the driver output resistance matches with the characteristic impedance of the interconnect. When evaluating noise peak voltage, the driver is modeled as a resistance for simplicity. Rise signals are input to all aggressors at the same timing and the peak voltage of the victim far-end noise is observed. In propagation delay evaluation, rise signals are input to all aggressors and the victim. We change the relative transition timing between the aggressors and the victim, whereas all aggressors make transitions at the same timing.

We use a transistor model for circuit simulation developed so that DC and AC characteristics match with ITRS2004 prediction [16]. Fundamental parameters such as threshold voltage, on-current, input capacitance and gate delay, are consistent with ITRS prediction. Layout parameters of standard cells of a 90nm CMOS technology are shrunk for other technologies according to gate length.

### C. Simulation setup in Scenario 2

In Scenario 2, transistor performance, supply voltage, dielectric constant of insulator are the same with those in Scenario 1. Interconnect width and thickness are set to 1$\mu$m and 0.9$\mu$m, and spacing is 1 or 4$\mu$m at all technology nodes based on the assumption that a high-performance thick interconnect layer will be provided in every technology. Interconnects are 1mm-long and not divided because the interconnect structure is unchanged. Other conditions on interconnects, such as interconnect layer and bus structure, in Scenario 2 are the same as those in Scenario 1.

## IV. PREDICTION RESULTS AND DISCUSSION

In this section, the impact of capacitive and inductive crosstalk noise at the future technology nodes is estimated

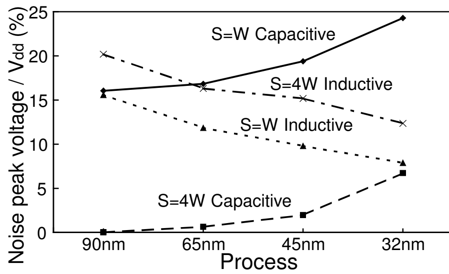


Fig. 5. Noise peak voltage normalized by $V_{dd}$ in Scenario 1.

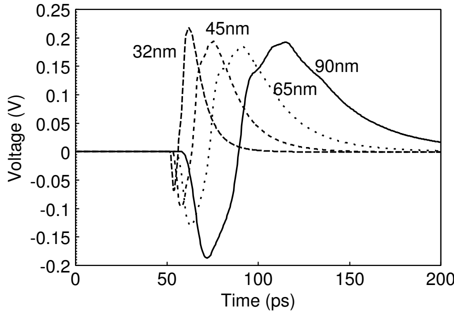


Fig. 6. Far-end noise waveform in Scenario 1, S=W structure.

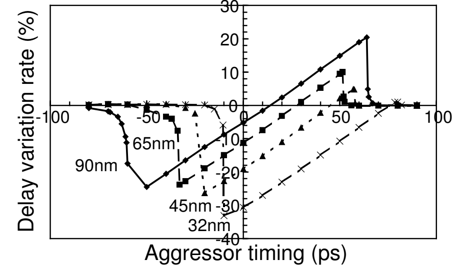


Fig. 7. Delay variation rate in Scenario 1, S=W structure.

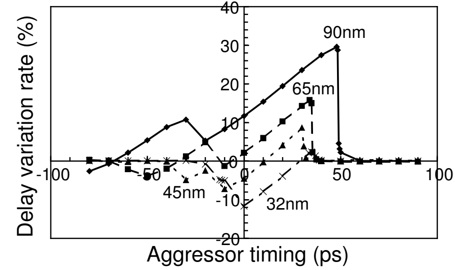


Fig. 8. Delay variation rate in Scenario 1, S=4W structure.

based on the assumed scenarios of process advancement explained in Section III.

## *A.* Scenario 1

Figure 5 shows noise peak voltage normalized by supply voltage in Scenario 1.

As process advances, the normalized peak voltage of capacitive crosstalk increases, and that of inductive crosstalk decreases. Shrinking interconnect spacing due to scaling enlarges coupling capacitance between interconnects relatively compared with grounded capacitance, which makes capacitive crosstalk significant. On the other hand, narrowing interconnect increases characteristic impedance of interconnects and decreases current, which results in reduction of inductive crosstalk noise. The high wire resistance also damps inductive noise.

Figure 6 shows the far-end noise waveforms in S=W structure. A gentle concave bump is caused by capacitive crosstalk and a sharp convex spike comes from inductive coupling. In the 90nm process, both capacitive and inductive crosstalk noises appear. On the other hand, in more advanced processes, capacitive crosstalk becomes dominant in S=W structure and comparable to inductive coupling in S=4W structure.

Figures 7 and 8 present delay variation rate in Scenario 1. Delay variation rate is defined as $D_{var}/D_{silent}$, where $D_{var}$ is delay variation and $D_{silent}$ is the delay when all aggressors are silent, i.e. no transitions at aggressors. The delay between 50% points of driver input and final receiver output is observed. In the current configuration of transition direction, delay increase is caused by inductive crosstalk noise, and capacitive crosstalk noise decreases the delay, because a noise waveform such as Fig. 6 is superposed on the rise transition of the victim. In S=W structure, the impact of capacitive crosstalk dominates that of inductive crosstalk as process advances. Inductive crosstalk is notably suppressed by technology progress even in S=4W structure. Delay increase due to inductive coupling noise is hardly found in 32nm technology. We therefore conclude that inductive coupling will be less important in the future advanced technologies.

## *B.* Scenario 2

Noise peak voltages normalized by supply voltage in Scenario 2 are shown in Fig. 9. The figure indicates that technology progress considerably increases the normalized peak voltage of inductive crosstalk noise because of faster switching speed in advanced processes and the non-scaled interconnect structure in Scenario 2. On the other hand, the effect of capacitive crosstalk is slightly reduced.

Figure 10 compares the normalized peak voltages of capacitive crosstalk noise simulated with RLC ladder model and with RC ladder model. The effect of capacitive crosstalk simulated with RC model increases as seen in Fig. 10, which is consistent with the relation between capacitive crosstalk and rise time of aggressor signal [13], [17]. Figure 10 implies that capacitive crosstalk noise is overwhelmed by inductive noise because consideration of inductance mitigates capacitive crosstalk.

Figure 11 and 12 present delay variation rate in Scenario 2. The impact of inductive crosstalk, which is observed as positive delay variation, is dominant. On the other hand, the increase of the maximum delay variation is small except the difference between 90nm and 65nm in S=W structure, i.e. considerable increase of normalized peak voltage in Fig. 9 is not directly related to delay variation. This is because the delay variation due to inductive crosstalk noise depends on both the noise peak voltage and the noise width.

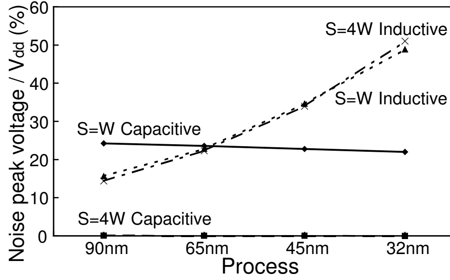


Fig. 9. Noise peak voltage normalized by $V_{dd}$ in Scenario 2.

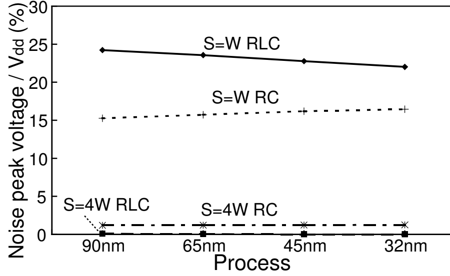


Fig. 10. Capacitive crosstalk noise peak voltage normalized by $V_{dd}$ in Scenario 2.

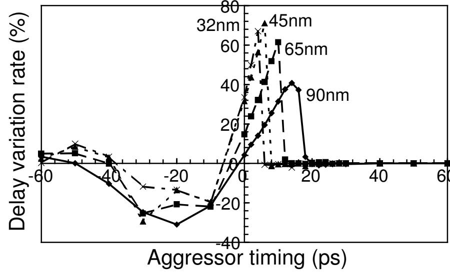


Fig. 11. Delay variation rate in Scenario 2, S=W structure.

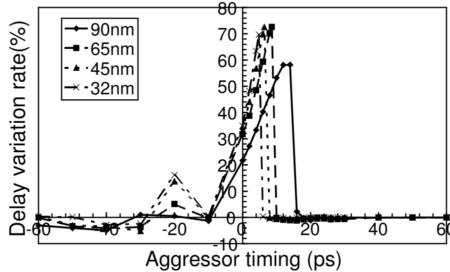


Fig. 12. Delay variation rate in Scenario 2, S=4W structure.

As far as either capacitive or inductive crosstalk extremely dominates the other, the period in which inductive crosstalk noise appears mainly depends on the difference between the times of flight for capacitive and inductive coupling as depicted in Figs. 2 and 3. A longer interconnect enlarges the differnce of the times of flight, and delay variation due to inductive crosstalk noise increases as shown in Fig. 13.

## V. WIRE CROSS-SECTIONAL AREA TUNING FOR INDUCTIVE CROSSTALK FREE INTERCONNECTS

Thick and wide interconnects generally provide short propagation delay, yet consume large interconnect resource. Our prediction in Section IV demonstrates that thick and wide

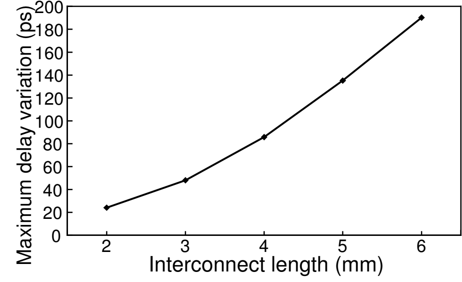


Fig. 13. Maximum interconnect delay variation vs. interconnect length.

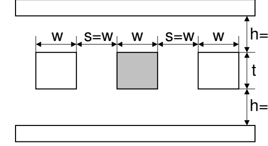


Fig. 14. Wire structure for determining aspect ratio.

interconnects in Scenario 2 involve larger inductive crosstalk, which may mean that interconnect delay is not nicely improved even with thick and wide interconnects in the future if special techniques such as differential signaling and shield insertion are not used. On the other hand, narrowing interconnect reduces delay uncertainty due to inductive crosstalk, because it increases wire resistance. However, unfortunately propagation delay also increases. This observation motivates us to explore the tradeoff between the worst-case delay considering inductive coupling noise and interconnect cross-sectional area. We here examine whether there is a wire cross-section that makes inductive coupling ignorable with a small penalty of delay increase. In other words, we evaluate the maximum performance of interconnects whose inductive coupling does not have a significant impact on timing design.

### A. Evaluation setup

We evaluate the interconnect propagation delay varying cross-sectional area from $1\mu m^2$ to $0.05\mu m^2$. The interconnect structure for RLC extraction and evaluation conditions are the same as Scenario 1 in Section III. S=4W structure is evaluated because we focus on the effect of inductive crosstalk. Drivers of aggressors and victim are 32X size inverters.

The aspect ratio of interconnect at each cross-sectional area value and process is decided such that the worst-case delay considering capacitive crosstalk is minimized. The worst-case delay is estimated by circuit simulation with an interconnect structure in Fig. 14. Resistance and capacitance of interconnects are calculated from formulas in [18]. In deriving the aspect ratio, the coupling capacitance is doubled for considering Miller effect of capacitive coupling for simplisity. From these consideration, the aspect ratios are set to 1.4-1.7.

### B. Experimental results and discussion

Figure 15 plots the relation between the worst-case delay and delay variation rate with 90nm and 32nm transistor models. In Fig 15, points with larger worst-case delay and smaller delay variation correspond to smaller cross-sectional

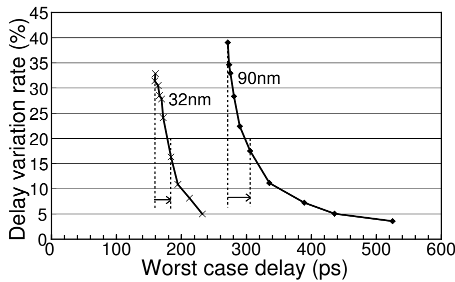

Fig. 15. The worst-case delay vs. delay variation rate when cross-sectional are is varied.

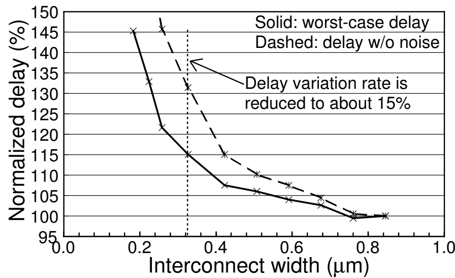

Fig. 16. Normalized delay vs. interconnect width. Absolute delay values of worst-case delay and delay without noise at $1\mu m^2$ area are 160 and 120ps respectively.

area. The worst-case delay is larger in narrower interconnects even if inductive crosstalk is considered. On the other hand, starting from the smaller worst-case value, i.e. large cross-sectional area, up to a certain point, narrowing interconnect notably reduces delay variation rate despite small degradation of the worst-case delay.

Figure 16 presents delay vs. interconnect width. In Fig. 16, delay w/o noise is the delay without crosstalk noises, and the worst-case delay means the delay degraded with the maximum delay variation due to inductive crosstalk noise. The delay shown in Fig. 16 is normalized by the delay with $1\mu m^2$ cross-sectional area. Please note that shrinking wire cross-section narrows interconnect width, and saves the interconnect resource. In Fig. 16, with a delay penalty of $15\%$, we can eliminate special design efforts to care for inductive coupling and improve routing efficiency by $61\%$ in the assumed 32nm technology.

Suppose here that the influence of inductive coupling can be ignored if the delay variation rate is smaller than $15\%$. The delay variation rate at $0.16\mu m^2$ area is about $15\%$ in 32nm process from Fig. 15. Compared with $1\mu$m-wide interconnects, the use of interconnect resource is reduced by $61\%$. When the crosstalk noise is not considered, shrinking interconnect degrades the delay by $31\%$ in Fig. 16. However, as a matter of fact, the worst-case delay considering inductive crosstalk noise increases only by $15\%$. This result indicates that narrowing cross-sectional area of high-performance interconnects can improve both interconnect efficiency and delay variation due to inductive coupling in spite of small deterioration of the interconnect propagation delay.

## VI. Conclusion

In this paper, we have presented the prediction of capacitive and inductive crosstalk effect in prospective processes. The peak noise voltage and delay variation due to crosstalk noise are evaluated in two scenarios, where interconnects scale down and do not scale. In the scenario with scaling, capacitive coupling will be more dominant and inductive coupling will be less important as technology advances. On the other hand, in the scenario without interconnect scaling, inductive coupling will be dominant.

The evaluation of the tradeoff between wire cross-sectional area and propagation delay considering inductive coupling noise is also presented. Shrinking the interconnect cross-section increases the propagation delay, but its increasing ratio is much moderated because higher wire resistance mitigates inductive coupling noise. An appropriate selection of interconnect cross-sectional area makes consideration of inductive coupling unnecessary with the small sacrifice of propagation delay.

## References


[1] D. Sylvester and K. Keutzer, “Getting to the bottom of deep submicron,” in *Proc. ICCAD*, pp. 203–211, 1998.

[2] K. Agarwal, D. Sylvester, and D. Blaauw, “A simplified transmission-line based crosstalk noise model for on-chip RLC wiring,” in *Proc. ASP-DAC*, pp. 858–864, 2004.

[3] Y. Massoud, J. Kawa, D. Macmillen, and J. White, “Modeling and analysis of differential signaling for minimizing inductive crosstalk,” in *Proc. DAC*, pp. 804–809, 2001.

[4] T. Sato, D. Sylvester, Y. Cao, and C. Hu, “Accurate in-situ measurement of noise peak and delay induced by interconnect coupling,” *IEEE JSSC*, Vol. 36, No. 10, pp. 1587–1591, Oct. 2001.

[5] A. Deutsch, et. al., “Modeling and characterization of long on-chip interconnections for high-performance microprocessors,” IBM Journal of Research and Development, Vol. 39, No. 5, pp. 547–567, 1995.

[6] Y. Ogasahara, M. Hashimoto, and T. Onoye, “Measurement of Inductive Coupling Effect on Timing in 90nm Global Interconnects,” in *Proc. CICC*, to appear.

[7] International Technology Roadmap for Semiconductors, “International technology roadmap for semiconductors 2004 update process integration, devices, and structures,” 2005.

[8] International Technology Roadmap for Semiconductors, “International technology roadmap for semiconductors 2004 update interconnect,” 2005.

[9] A. Sakai, T. Yamada, Y. Matsushita, and H. Yasuura, “Reduction of coupling effects by optimizing the 3-D configuration of the routing grid,” *IEEE trans. on VLSI Systems,* Vol. 11, No. 5, pp. 951–954, Oct. 2003

[10] Y. Massoud, J. Kawa, D. MacMillen, and J. White, “Modeling and analysis of differential signaling for minimizing inductive crosstalk” in *Proc DAC,* pp. 804–809, 2001.

[11] R. Kumar, “Interconnect and noise immunity design for the Pentium 4 processor,” in *Proc. DAC,* pp. 938–943, 2003.

[12] C. Cheng, J. Lillis, S. Lin, and N. H. Chang, “Interconnect analysis and synthesis,” Wiley-Interscience Publication, 2000.

[13] J. Cong, D. Z. Pan, and P. V. Srinivas “Improved crosstalk modeling for noise constrained interconnect optimization,” in *Proc. ASP-DAC*, pp. 373–377, 2001.

[14] H. B. Bakoglu, “Circuits, interconnections, and packaging for VLSI,” Addison-Wesley Publication, 1990.

[15] Synopsys Corp., “Raphael interconnect analysis program reference manual,” June 2004.

[16] http://www.tamaru.kuee.kyoto-u.ac.jp/˜tsuchiya/tr-model.html.en

[17] J. M. Rabaey, A. Chandrakasan, and B. Nikolic, “Digital integrated circuits a design perspecitve,” Pearson Education, 2003.

[18] http://www.eecs.umich.edu/˜dennis/bacpac/index.html